



International Journal of Engineering Researches and Management Studies

CORROSION BEHAVIOR OF CU-AL-BE SHAPE MEMORY ALLOYS IN FRESH WATER, SEA WATER AND HANKS SOLUTION.

Prashantha S^{*1}, Shivasiddaramaiah.A.G², U S Mallikarjun³, S M Shashidhara⁴

^{1&2}Asst.Prof. Department of Mechanical Engineering, Siddaganga Institute of Technology, Tumkur-572 103, Karnataka, India

³Prof. Department of Mechanical Engineering, Siddaganga Institute of Technology, Tumkur-572 103, Karnataka, India

⁴Dean(S.W), Sridevi Institute of Engg. & Technology, Tumkur-572 106, Karnataka, India

ABSTRACT

Ternary alloy of Cu-Al-Be (80-90 % Cu, 8-10 % Aluminum & 0.1-0.5 % Beryllium) was prepared using ingot metallurgy route. The prepared alloys were tested for its SME using Bend test. The corrosion behavior of the SMA investigated in various corrosion media. It was observed that the alloy undergoes Intergranular corrosion. The addition of little amount of beryllium was effective to reduce the intergranular corrosion. It was found that, the small amount of beryllium addition prevents the intergranular corrosion which is possibly due to the diffusion of beryllium atoms into grain boundaries, which in turn deactivates the grain boundaries.

Keywords: Shape Memory Alloys, Shape Memory Effect, corrosion tests, Corrosion Behavior, Intergranular corrosion.

I. INTRODUCTION

During recent time, smart materials and structures have received increasing attention because of their great scientific and technological significance in various applications. Shape memory alloys are the most important branch from the smart and/or intelligence materials. The term "Shape memory alloys" refers to that group of metallic materials which have the ability to return to some previously defined shape or size when subjected to appropriate thermal cycle [1].

Ni-Ti Shape Memory Alloys is well known and is being used practically as a shape memory alloy since many years. Among many alloy systems which exhibit shape memory effect, Ni-Ti, Cu-Al-Ni and Cu-Zn-Al shape memory alloys have over the years been studied extensively. The Ni-Ti shape memory alloys in particular are used extensively in many engineering and bio medical applications. Some of the disadvantages that these alloys suffer from are low transformation temperature, difficulty in production and processing and high cost.

Copper based shape memory alloys, on the other hand are easier to produce and process, and are also less expensive. But these copper based SMAs are brittle and cannot, therefore, be processed easily. Attempts to improve the ductility of these polycrystalline copper based shape memory alloys by grain refinement have only resulted in limited success. But it has been found by recent studies that the Cu-Al-Mn SMAs exhibit good ductility because of their parent phase has L21 structure with a low degree of order [2].

In Cu-Al-Be ternary alloy, the beta-phase region of Cu-Al binary alloy system was extended to lower aluminum side by the addition of beryllium and the Ms-temperature will be lowered by the addition of beryllium [3].

Copper based Shape Memory Alloys can be used in various applications such as valves, pipes, fasteners etc. In many of these applications, the SMA's are exposed to various corrosive medias. Almost about 75 % of the degradation of the material and failure with change in its properties in various applications can be attributed to corrosion.

In the present work the effect of various corrosion media like fresh water, Sea water and Hanks solution on the Cu-Al-Be SMA's was investigated.



International Journal of Engineering Researches and Management Studies

II. EXPERIMENTAL PROCEDURE

Alloy preparation

Cu-Al-Be SMA's with 2 - 15 wt.% of Aluminum and 0.1 – 0.5 wt.% of Beryllium were chosen for the present study, as the alloys exhibit β -phase at high temperatures and manifest shape memory effect on quenching to form martensite in this composition range. The alloys were prepared by using pure Copper; Aluminum and Beryllium cut from the respective metal ingots, and taken in the right quantities to weigh 100 gm of the alloy and were melted together in an induction furnace under inert atmosphere. The molten alloy was poured into a cast iron mould of dimensions 150mm×100mm×5mm and allowed to solidify. The ingots were then homogenized at 900°C for 6hour. The compositions of the cast alloys were determined using an integrally coupled plasma-optical emission spectrophotometer. The alloy samples were then hot rolled at 900°C to a thickness of 1 mm. The rolled samples were betaized for 30min at 900°C and step quenched into boiling water (100°C) and then quenched into a water bath at room temperature (~30°C) to avoid martensitic pinning effect. The microstructure and morphology of martensites formed were studied using an optical microscope. The transformation temperatures were determined using differential scanning calorimeter (DSC) by heating/cooling the samples at the rate of 10°C/min. The phases present in the polycrystalline samples at room temperature were determined by X-ray diffraction.

Determination of shape memory effect (SME)

The shape memory effect was evaluated by bending the rolled specimen with dimensions of 1×4×50mm³ (thickness ×width ×length) at room temperature. The specimens were bent around a mandrel of known diameter at room temperature by the application of load. During recovery treatment the bent samples were heated to above A_f temperature of the alloy and then cooled to room temperature. After recovery treatment the recovered angle (θ) was measured. A schematic diagram showing the procedure to conduct bend test is illustrated in Figure 1.

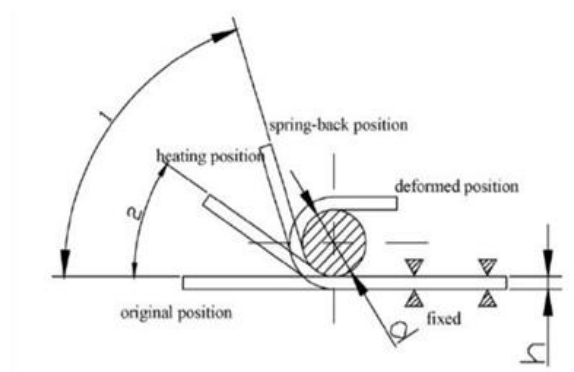


Figure1: Schematic View of Bend Test [6].

Corrosion test

Corrosion is an electrochemical process in which a metal reacts with its environment to form an oxide or other compound. The cell which causes this process has three essential constituents: an anode, a cathode and an electrically conducting solution. The anode is the site at which the metal is corroded, the electrolyte solution is the corrosion medium, and the cathode forms the other electrode of the cell and is not consumed in the corrosion process.

An Investigation of the corrosion behavior of Cu-Al-Be SMAs with varying Al and Be contents was carried out in different corroding media. Flat rectangular alloy specimens (20 mm x 20 mm x 1 mm) were cut from the rolled alloy samples for the test. These specimens were finely polished using emery papers and then polished with Al₂O₃ powder and diamond paste. First the micrographs of the polished surfaces were imaged using the optical microscope before subjecting them to corrosion studies. Depending on the usual applications of SMAs, three corrosion media i.e. fresh water, sea water and hanks solution (simulates the body solution) were selected for the study. Sea water was prepared as per ASTM D 1141-98 (Reapproved 2003) and the hanks solution was prepared as per the literature [Zheng et al., 2006]. In practical applications, as the alloys are exposed to the



International Journal of Engineering Researches and Management Studies

corrodant for a longer period of time they are prone to pitting corrosion. Therefore pitting corrosion potential of the alloys was determined using an electrochemical cell with potentiostat. The schematic diagram of the setup and a photograph of the setup are shown in Fig. 2. (a) and (b). The standard test cell requires 200 ml of test solution. The sample was then placed in the cell and the electrodes were kept in their respective positions as shown in Fig. 2(b). The area of exposure of the sample to the electrolyte solution is 1 cm². The reference electrode and counter electrode were placed in their respective holders and connected to the potentiostat. A saturated calomel electrode was used as the reference electrode and a platinum electrode as the counter electrode during the test. The voltage in the circuit and the current values are measured and the output is obtained in the form of E-I plot. The corrosion potentials E_(corr) and E_(pit) were determined for all the alloy samples considered. The microstructure of the surface of the alloy specimens after corrosion was imaged using an optical microscope (OM) and analyzed. The chemical composition of the corrosion products formed at the corroded surface was obtained using a spot EDAX of the corroded surface using SEM

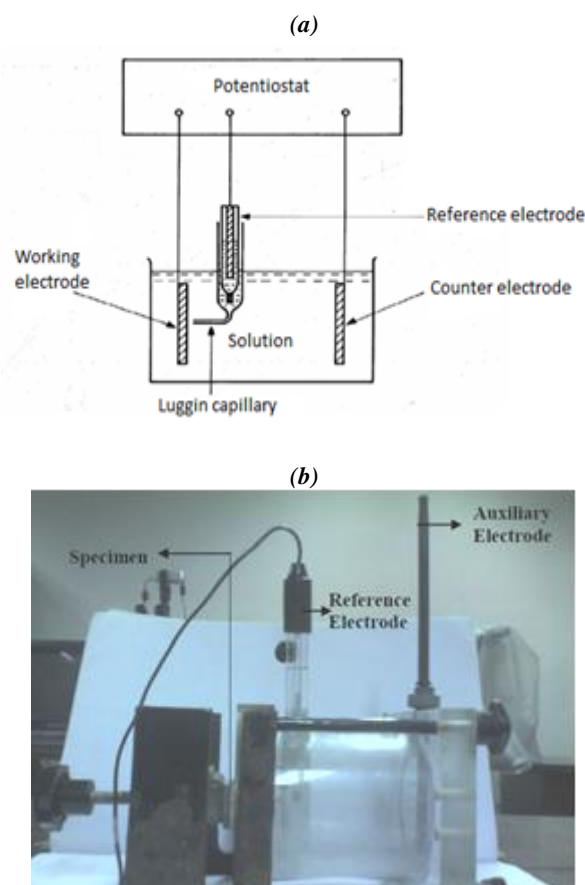


Figure2 :(a) Schematic diagram of an electrochemical cell, (b) Photograph of experimental setup for corrosion studies.

Working electrode – Specimen.

Reference electrode – saturated calomel electrode.

Counter / Auxiliary electrode – A conductor that completes cell circuit(Platinum)

Preparation of different corrosion medias

The ocean sea water was prepared as per the ASTM D 1141-98 (Reapproved 2003) standards.

Preparation of Hank's solution

The Hanks's solution which simulates the body solution is prepared as per the literature available. It is prepared by dissolving the following salts (Table 1) in 1 L of distilled water. The pH was maintained at 7.2 at a temperature of 37°C [Zheng et al., 2006].



Table 1. Chemical composition of Hank's Solution (g/l).

NaCl	8.00g/L
Glucose	1.00g/L
KCl	0.40g/L
MgCl ₂ .6H ₂ O	0.10g/L
Na ₂ HPO ₄ .2H ₂ O	0.06g/L
KH ₂ PO ₄	0.06g/L
MgSO ₄ .7H ₂ O	0.06g/L
CaCl ₂	0.14g/L
NaHCO ₃	0.35g/L

III. RESULTS AND DISCUSSION

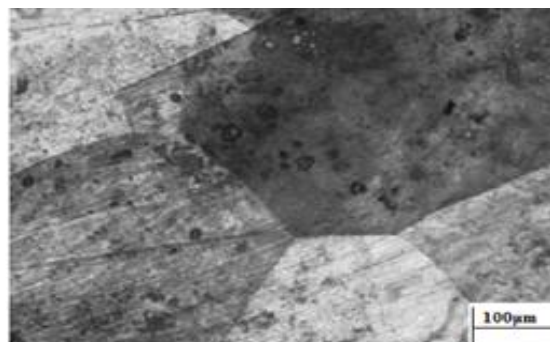
Compositional analysis

The compositions of the cast alloys were determined using Perkin Elmer Integrally Coupled Plasma-Optical Emission Spectrophotometer (ICP-OES), which is capable of determining the compositions up to the second decimal place. For composition analysis 1 g of the alloy sample taken from the middle portion of the homogenized ingots was completely dissolved in concentrated HNO₃. It was diluted to a ratio of 1: 20 using distilled water before using the solution in the ICP-OES. It could be further diluted as per the requirement in the instrument using an online diluter. The solution was aspirated in the instrument using a plasma source and was analyzed by optical emission spectrophotometry for the chemical composition.

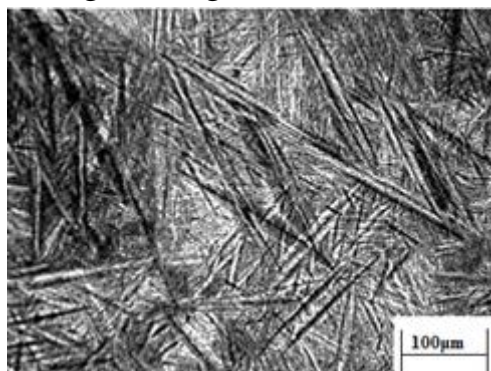
From the spot EDAX analysis, intermetallic particles were found and there is an increase in amount of aluminum in the precipitate, while the concentration of Beryllium in the precipitate is less.

Microstructure

Samples were cut and were mechanically polished in emery sheets of 200-2000 grit size followed by cloth polishing with alumina paste to get very fine polished surface. Samples were etched in an etchant solution of K₂Cr₂O₇ - 8ml H₂SO₄ - 2ml HCl - 100ml H₂O. These samples were examined under upright optical microscope (Olympus-Japan) using 50X magnification



(a)



(b)

Figure 3. Micrograph of the Cu-Al-Be alloy (a) Austenite (b) Lath martensite.

The Micrograph of as cast SMA having the Austenite structure is as in Fig.3 (a) and the micrograph of room temperature martensite phase of the Cu-Al-Be SMA is as in Fig.3 (b). The micrograph clearly exhibits the formation of twinned martensite, which leads to good shape memory characteristics.

Shape memory effect

Table 2. Estimation of Percentage SME exhibited by the studied Cu-Al-Be SMA after Bend Test

Sample	Diameter in mm	Thickness in mm	Angle recovered on heating (θ_m)	SME %
CAB 1	32	1	60	65
CAB 2	32	1	72	81
CAB 3	32	1	89	98
CAB 4	32	1	80	88
CAB 5	32	1	78	86
CAB 6	32	1	88	98
CAB 7	32	1	85	94
CAB 8	32	1	90	96
CAB 9	32	1	90	100

It can be observed that the alloys exhibit good shape memory effect which varies from 65 % to 100 % strain recovery by SME. The strain recovery by SME depends upon the volume of Martensite transformed and which transforms again back to austenite.

Corrosion test

Table 3. Chemical Composition and Corrosion Potentials of Cu-Al-Be SMA's

Alloy ID	Chemical Compositions in (wt. %)			$E_{(corr)}$ (mV)		
	Cu	Al	Be	FW	HS	SW
CAB 1	88.08	11.5	0.42	- 98.5	- 241.2	- 262.3
CAB 2	87.08	12.5	0.42	- 94.6	- 232.2	- 240.5
CAB 3	86.08	13.5	0.42	- 92.4	- 228.4	- 232.7
CAB 4	88.05	11.5	0.45	- 90.5	- 230.0	- 258.5

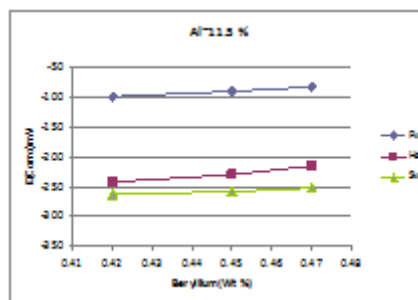


International Journal of Engineering Researches and Management Studies

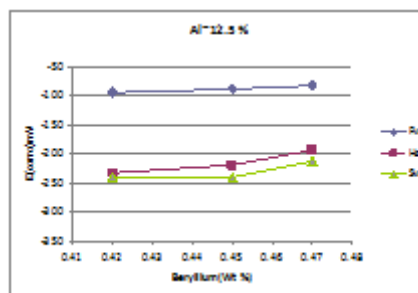
CAB 5	87.05	12.5	0.45	-	-	-
CAB 6	86.05	13.5	0.45	87.7	218.6	239.8
CAB 7	88.03	11.5	0.47	-	-	-
CAB 8	87.03	12.5	0.47	84.6	187.9	210.1
CAB 9	86.03	13.5	0.47	82.3	214.5	252.2
				81.4	193.6	212.6
				79.2	182.7	197.2

It is observed that the addition of Aluminum to copper based alloys improves the corrosion resistance when they are exposed to corrosive environments. Beryllium-copper resists the Marine fouling, makes it suitable for sea applications because corrosion of the alloy releases the cupric ions which are toxic to fouling organisms [7].

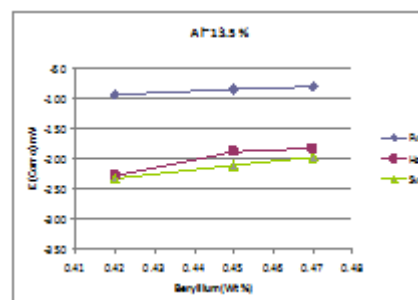
The polarization curves were generated using a potentiostat, using the Saturated Calomel reference Electrode and the potential was measured (mV) with a sweep rate of 25 mV/min and Start Potential of -250 mV and Reverse Potential of 2000 mV.



(a)



(b)

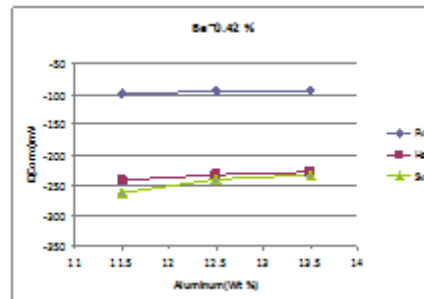


(c)

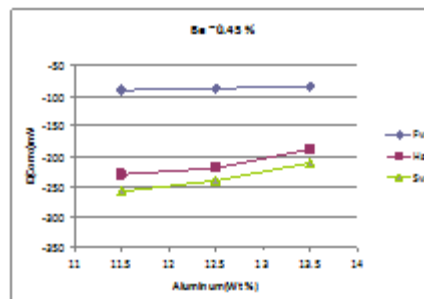


International Journal of Engineering Researches and Management Studies

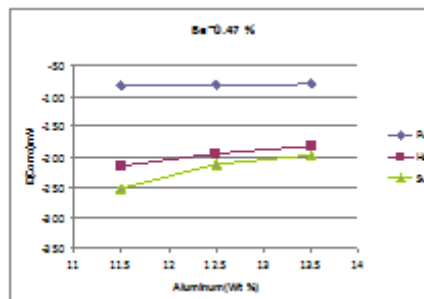
Figure 4. Variation in Corrosion potential $E_{(corr)}$ with the variation in Beryllium content when that of Aluminum was maintained more or less constant. (a) % Al is 11.5. (b) % Al is 12.5. (c) % Al is 13.5.



(a)



(b)



(c)

Figure 5. Variation in Corrosion potential $E_{(corr)}$ with the variation in Aluminum content when that of Be was maintained more or less constant. (a) % Be is 0.42 (b) % Be is 0.45 (c) % Be is 0.47

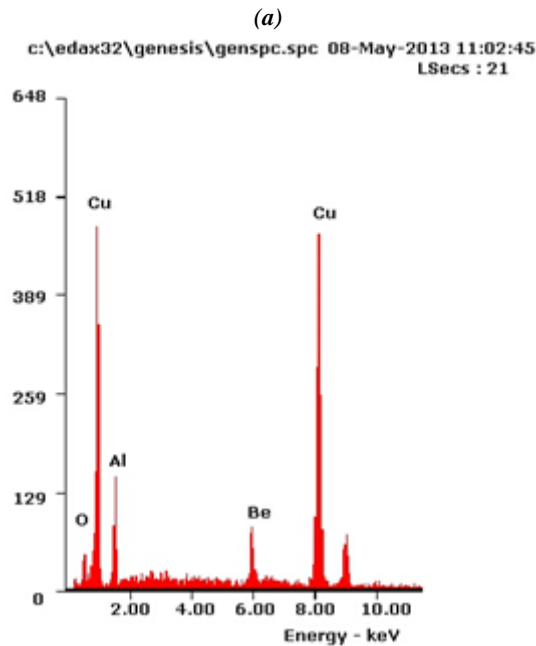
Fig. 4 shows the plots of variation in the corrosion potential $E_{(corr)}$ with the variation in Beryllium concentration when the concentration of aluminum was maintained more or less constant in the alloys. Fig. 5 shows the plots of variation in corrosion potential $E_{(corr)}$ with the variation in the amount of aluminum when that of Beryllium was maintained more or less constant. It can be observed that an increase in the Aluminum and Beryllium content increases the corrosion resistance of the alloys. Aluminum reacts with oxygen present in the surrounding medium to form a thin, tough surface layer of alumina (aluminum oxide) which acts as a barrier to the corrosion of the copper-rich alloys, thereby increasing their corrosion resistance. On the other hand, beryllium reacts and dense oxide film is formed on the surface of beryllium which acts as protective coating and makes the alloy resistance to corrosion, leading to an increase in the corrosion resistance of the alloys. It is well supported by the spot EDAX of the corroded surface showing mainly the presence of oxygen concentration at the surface. It may be due to the diffusion of beryllium atoms into the grain boundaries acting as a barrier to intergranular corrosion.

The EDAX analysis of the alloy samples in various corrosive media at the corroded surface are as in Fig.6. The EDAX analysis of the alloy shows that, the alloy exposed to fresh water form oxides of Al and Be at the

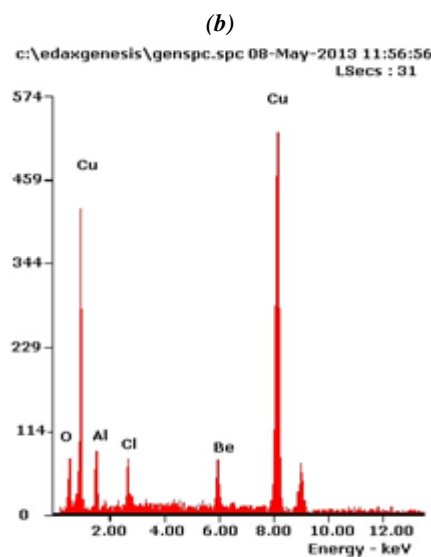


International Journal of Engineering Researches and Management Studies

corroded surface. The increased Be content leads to increase in corrosion resistance of the alloy. The alloys exposed to Hank's solution and Sea water also exhibits similar trend. In these alloys, the amount of oxygen at the corroded surface was increased and that of Al reduced. The formation of chlorides could also be noticed, which is due to the presence of different salts in the corrosion media. The initial resistance to corrosion was due to the formation of an oxide layer of Al.

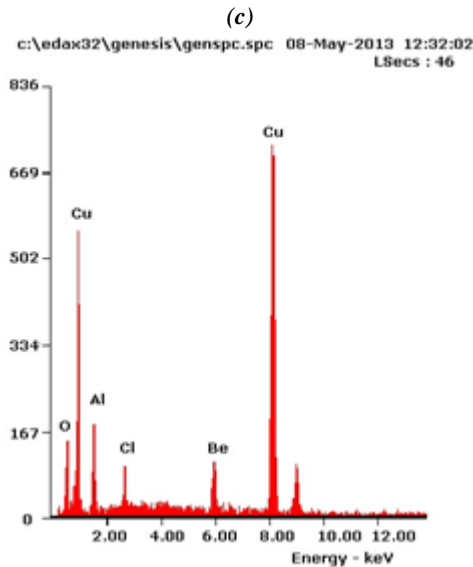


<i>Element</i>	<i>Wt %</i>	<i>At%</i>
<i>O K</i>	<i>7.42</i>	<i>21.14</i>
<i>Al K</i>	<i>11.59</i>	<i>19.12</i>
<i>Be K</i>	<i>0.46</i>	<i>1.72</i>
<i>Cu K</i>	<i>80.53</i>	<i>58.02</i>





Element	Wt %	At%
O K	9.15	26.07
Al K	9.92	15.84
Cl K	3.22	3.81
Be K	0.44	1.60
Cu K	77.27	52.68



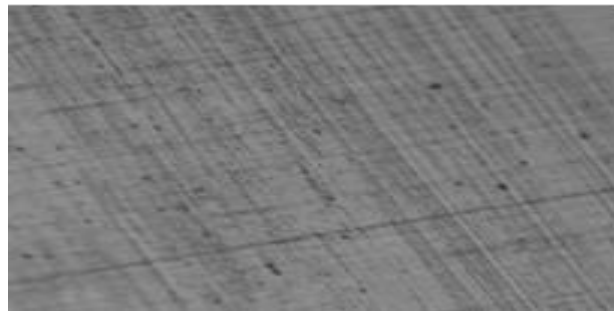
Element	Wt %	At%
O K	11.28	31.02
Al K	9.27	14.92
Cl K	3.14	3.64
Be K	0.40	1.47
Cu K	75.91	48.95

Figure 6. EDAX analysis of the Cu-Al-Be alloy after corrosion in various corrosive media at the corroded surface (a) Spectrum Label in fresh water. (b)Hanks solution.(c)Sea water.

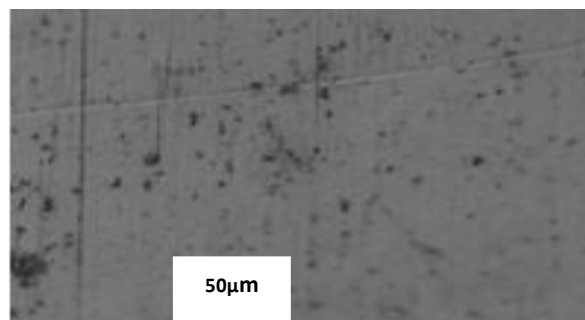
The optical micrographs of the alloy sample CAB1 and CAB 3 before and after corrosion in different corrosion media are as in Fig.7 and 9. Though the alloys exhibit good corrosion resistance, i.e. high corrosion potential values, it is observed that after the depletion of the passive layer a large number of pits were formed. It completely deteriorates the materials so that they could not be used further. The composition analysis by EDAX of the corroded surface shows that the corrosion is mainly by the formation of oxides and chlorides.

The optical micrograph of the alloys exhibiting the surface of the alloy CAB1 before and after corrosion is as in Fig.7. A complete degradation of the surface of the alloy with formation of pit can be observed.

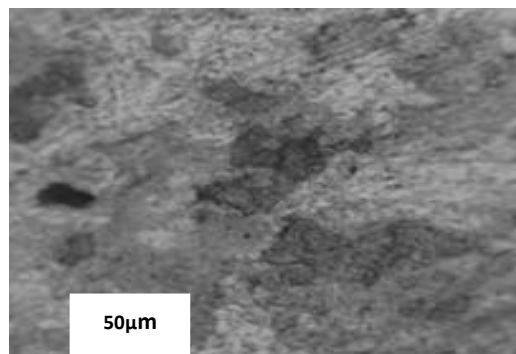
The Tafel plots of the alloy CAB1 in three corrosion media under consideration is as in Fig. 8. The potentials where the alloy begins to corrode given by $E_{(corr)}$ and where the pit formation begins given by $E_{(pit)}$ can be observed in these tafel plots



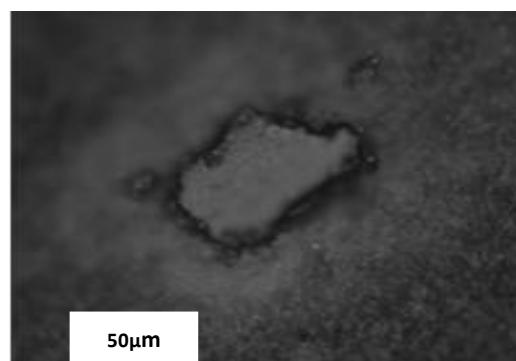
(a)



(b)



(c)



(d)

Figure 7. Optical micrographs of the alloy sample CAB 1 at resolution 20X: (a) before corrosion; (b) after corrosion

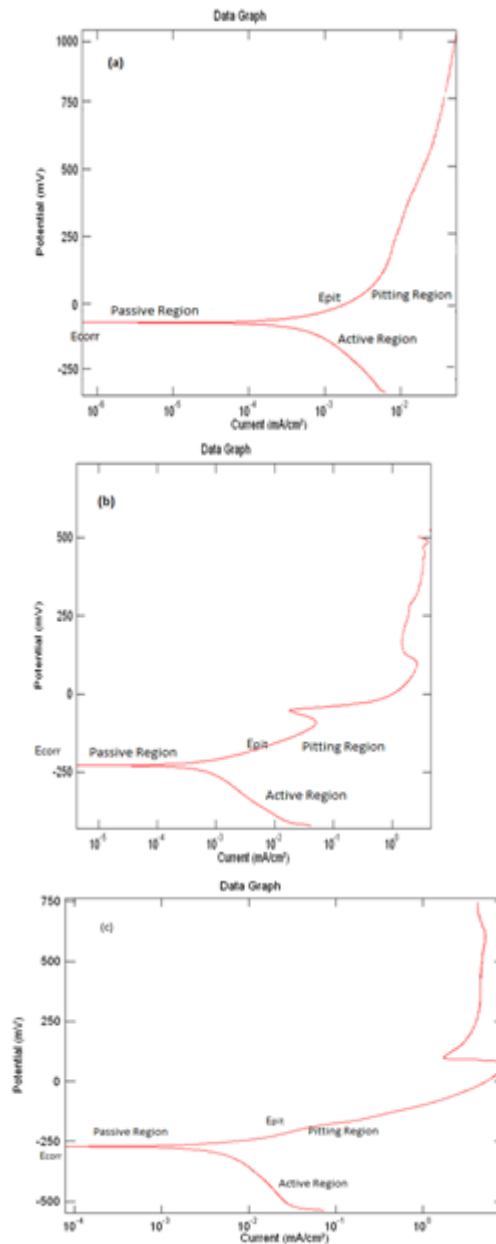
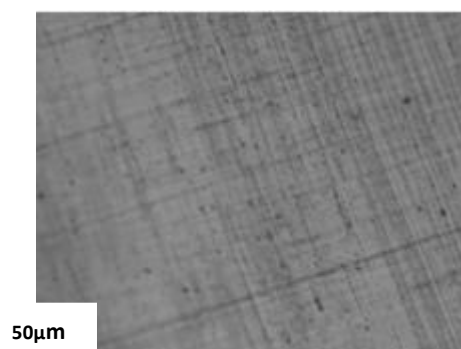


Figure.8. Tafel plots for the alloy sample CAB 1 in three corrosion media (a) fresh water (b) Hanks solution (c) sea water



(a)

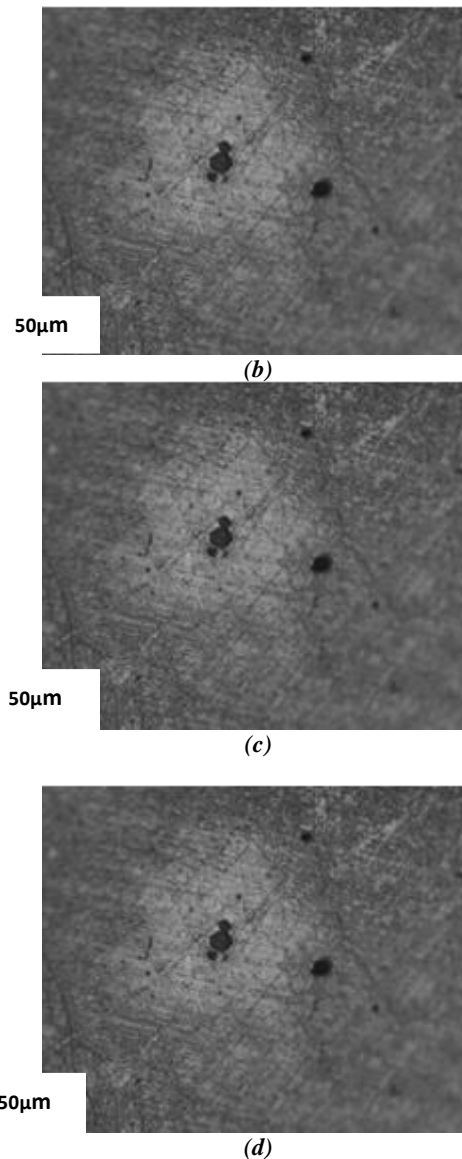


Figure 9. Optical micrographs of the alloy sample CAB 3 at resolution 20X: (a) before corrosion ; (b) after corrosion in fresh water ; (c) after corrosion in hanks solution ; (d) after corrosion in sea water.

Fig. 9 and Fig. 10 shows the optical micrographs of the alloy and tafel plots for the sample (CAB 3) respectively. It is clear that current density in fresh water is high compared to Hanks solution and sea water which demonstrates that shape memory alloys have more corrosion resistance due to hyper elastic behavior of polycrystalline structure.

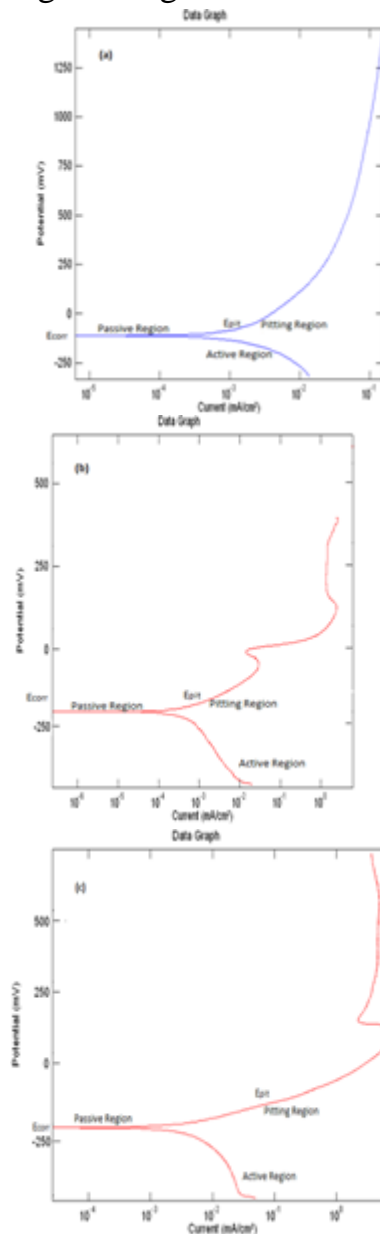


Figure 10. Tafel plots for the alloy sample CAB 3 in three corrosion media (a) Fresh water (b) Hanks solution (c) Sea water.

From the micrographs, it can be observed that the alloys initially undergo uniform corrosion and after some time there is formation of pits. Compared to corrosion in fresh water and Hanks solution, more number of wider and deeper pits are observed in Sea water corrosion due to the depletion of the passive layer indicating Sea water has a higher effect on the alloy samples. It is same in case of Hank's solution also.

It is observed that the corrosion potential E_{corr} and E_{pit} of the alloy increases with the addition of Beryllium. The alloy has greater susceptibility to pitting corrosion in Sea water and Hanks solution compared to Fresh water, because of this it may not be suitable for use in Marine Bio medical applications.



International Journal of Engineering Researches and Management Studies

IV. CONCLUSION

1. In the present work, it can be observed that the corrosion rate of the Cu-Al-Be SMA is less in fresh water compared to hanks solution and sea water.
2. Addition of small amount of beryllium in the alloy enhances the corrosion resistance of the Cu-Al-Be SMA.
3. As the composition of the alloys also changes due to corrosion it can be presumed that it changes the inherent shape memory properties of the alloys. Therefore while using this alloy for any application careful attention has to be given to this aspect.
4. The addition of small amount of beryllium prevents the intergranular corrosion which is due to diffusion of beryllium atoms into grain boundaries by vacancy mechanism.
5. Beryllium carbide impurities in beryllium will react with water in the atmosphere to form beryllium oxide.
6. The increase in corrosion potential with the addition of beryllium to the alloy suppresses the electrochemical activity of the alloy.
7. The alloy exhibit good corrosion resistance in fresh water compared to Sea water and Hank's solution.

REFERENCES

- [1] R.Noecker, *Shape memory materials "Martensitic structures, Metallography and Microstructure , Vol.9,ASM Hand book , ASM international , 2004.*
- [2] U. S. Mallik and V. Sampath, "Influence of Aluminum and Manganese Concentration on the Shape Memory Characteristics of Cu-Al-Mn Shape Memory Alloys," *Journal of Alloys and Compounds, Vol. 459, No. 1-2, 2008, pp. 142-147.*2007.
- [3] A.Higuchi , K. Suzuki , Y. Matsumoto , K. Sugimoto , S. Komatsu and Y. Nakamura *Journal De Physique, Colloque C4, Supplement 12, Tome 43, (1982) C4-767-771.*
- [4] S.Otani , Hiraishi H, Midorikawa M. "Development of smart systems for building structures". *Proceedings of SPIE 2000;3988:2-9.*
- [5] M. Indirli et al. "Demo application of shape memory alloy devices: the rehabilitation of S. Georgio Church Bell Tower. *Proceedings of SPIE2001;4330:262-72.*
- [6] Feng Chen, Bing Tian, Yuxiang Tong, Yufeng Zheng. "Transformation behavior and Shape Memory Effect of Co- Al alloy". *International Journal of Modern physics, Vol. 23, Nos. 6 & 7 (2009) 1931-1936.*
- [7] F.L. Laque, *Marine Corrosion, Wiley & Sons, Inc., New Yorkpp.130-2,308-11(1975).*